Geomechanics and Engineering, *Vol. 25, No. 2 (2021) 143-157*
DOI: https://doi.org/10.12989/gae.2021.25.2.143

Mechanical properties and microstructures of stabilised dredged expansive soil from coal mine

Thanakorn Chompoorat[1a], Suched Likitlersuang[*2], Suwijuck Sitthiawiruth[3b], Veerayut Komolvilas[2c], Pitthaya Jamsawang[4d] and Pornkasem Jongpradist[5e]

[1]*Department of Civil Engineering, School of Engineering, University of Phayao, Phayao, 56000, Thailand*
[2]*Centre of Excellence in Geotechnical and Geoenvironmental Engineering, Department of Civil Engineering, Faculty of Engineering, Chulalongkorn University, Bangkok 10330, Thailand*
[3]*Department of Civil Engineering, Faculty of Engineering, Chulalongkorn University, Bangkok 10330, Thailand*
[4]*Soil Engineering Research Center, Department of Civil Engineering, King Mongkut's University of Technology North Bangkok, Bangkok 10800, Thailand*
[5]*Department of Civil Engineering, Faculty of Engineering, King Mongkut's University of Technology Thonburi, Bangkok 10140, Thailand*

(Received January 26, 2021, Revised April 4, 2021, Accepted April 6, 2021)

Abstract. Expansive soil is the most predominant geologic hazard which shows a large amount of shrinkage and swelling with changes in their moisture content. This study investigates the macro-mechanical and micro-structural behaviours of dredged natural expansive clay from coal mining treated with ordinary Portland cement or hydrated lime addition. The stabilised expansive soil aims for possible reuse as pavement materials. Mechanical testing determined geotechnical engineering properties, including free swelling potential, California bearing ratio, unconfined compressive strength, resilient modulus, and shear wave velocity. The microstructures of treated soils are observed by scanning electron microscopy, x-ray diffraction, and energy dispersive spectroscopy to understand the behaviour of the expansive clay blended with cement and lime. Test results confirmed that cement and lime are effective agents for improving the swelling behaviour and other engineering properties of natural expansive clay. In general, chemical treatments reduce the swelling and increase the strength and modulus of expansive clay, subjected to chemical content and curing time. Scanning electron microscopy analysis can observe the increase in formation of particle clusters with curing period, and x-ray diffraction patterns display hydration and pozzolanic products from chemical particles. The correlations of mechanical properties and microstructures for chemical stabilised expansive clay are recommended.

Keywords: expansive soil; mechanical properties; microstructure; ground improvement; road material

1. Introduction

Clay that displays volume changes with variation in its water content is known as expansive clay (Nelson and Miller 1997). Expansive soils defined as geological formation problem are found in many countries of the world such as USA, China, Brazil (Jiang *et al*. 2013, Khan *et al*. 2017, Freitas *et al*. 2020). Such volume changes can cause damage to structures built atop the expansive clay, leading to financial loss (Wayne *et al*. 1984, Avsar *et al*. 2009). Clays, particularly those classified as low plasticity clay (CL) and high plasticity clay (CH), are expansive (Komin and Ogata 1996, Khattab *et al*. 2007, Souza and Pejon 2020) and experience softening and a decrease in strength when saturated (Ghose and Subbarao 2007). As such, buildings built on top of expansive clays are subject to increased stress levels and damages due to volumetric changes in the clay with changing water content.

For more than two decades, Thailand has undergone tremendous development in its infrastructure. However, the issue of expansive clays has not been considered in the design and construction of some of these infrastructure projects. As a result, increased stress and damage has been seen in some structures in northern Thailand; in some worst cases, some houses and roads were destroyed.

The Mae Moh Lignite mine is the largest mine in Thailand and the largest open-pit lignite mine in Southeast Asia, operated under the responsibility of the Electricity Generating Authority of Thailand (EGAT). The mine is also the main fuel source in Thailand, producing 2,400 MW or 8% of the electricity consumed in the country. Some parts of Mae Moh mine are situated on a layer of expansive clay known as Mae Moh yellow clay, which has a shallow depth of around 3 to 5 m below ground surface. This expansive soil layer experiences shrinkage and swelling with seasonal changes of clay moisture and has previously caused stability and deformation problems for pavement structures in the mine. Recently, the Mae Moh mine began planning a road construction atop the expansive soils in the mining area to improve its transportation network and facilitate access for

∗Corresponding author, Professor
E-mail: fceslk@eng.chula.ac.th
[a]Ph.D.
[b]M.Eng
[c]Ph.D.
[d]Ph.D.
[e]Ph.D.

ISSN: 2005-307X (Print), 2092-6219 (Online)

passengers and businesses. In addition, this expansive soil has never been involved in construction before. The construction of the road embankment has become a challenge for geotechnical engineers, causing some to consider shallow cement and lime mixing methods to improve the expansive soil's properties.

Many studies in literature describe improving the physical and engineering properties of expansive clay by addition of lime, ordinary Portland cement (OPC), fly ash or other stabilisers, mostly from a macroscopic point of view (Osinubi 2000, Phanikumar 2009, Sharma *et al*. 2012, Mutaz and Dafalla 2014, Zaimoglu *et al*. 2015, Jamsawang *et al*. 2017, Guidobaldi *et al*. 2017, Jiang *et al*. 2017, Wei *et al*. 2019, Sun *et al*. 2020). In addition, several researches also studied the cyclic behaviour of clay and sand (Thay *et al*. 2013, Chompoorat and Likitlersuang 2016, Mase *et al*. 2019). Mixing clays with stabilisers leads to reactions that affect cation exchange and pozzolanic reactions that stabilise the clay (Al-Mukhtar *et al*. 2012). While cation exchange quickly stabilises the clay and improves its plastic and compaction properties, pozzolanic reactions increase the shear strength of clay by bonding close particles together after some curing time (Arabi and Wild 1986, Bell 1996, Boardman *et al*. 2001, Rao and Shivananda 2005). Studies in literature have quantified the improvement of clay properties according to the Atterberg limits and other soil properties such as the volume change, shear strength, and coefficient of permeability of the improved expansive clay (Diamond and Kinter 1965, Brandl 1981, Locat *et al*. 1990, Sivapullaiah *et al*. 2000, Por *et al*. 2015, 2017, Bozbey *et al*. 2021).

The treatment of clay with lime is of particular interest around the world because lime usage oftentimes employs local materials and involves low costs of lime, while the clay is improved in its technical capabilities and competitiveness. Mixing lime into clay causes four types of reactions: cation exchange, flocculation, carbonation, and pozzolanic reactions. Cation exchange occurs between the cations affixed to clay surface particles and the calcium cation (Ca^{2+}) of the lime; it causes the clay particles to get closer to each other due to flocculation and attraction. Flocculation is primarily accountable for the changes in engineering properties when lime is added to clays; adding lime causes a marked decrease in a clay's swelling potential, liquid limit (LL), plasticity index (PI), and maximum dry density of the soil, while the optimum water content, shrinkage limit, and strength are increased (Croft 1967, Alrubaye *et al*. 2018, Türköz 2019). The same results are seen when clay is treated with cement, where the clay's LL, PI, and swelling potential decrease, while the shrinkage limit (SL) and shear strength increase (Nelson and Miller 1997, Ghiyas and Bagheripour 2020). Finally, it has been found that applying cement stabilisation to soils promotes the creation of cementitious bonds between calcium silicate or aluminate hydration products with soil particles which further promotes soil stability (Chompoorat and Likitlersuang 2016, Julphunthong *et al*. 2018, Thomas and Rangaswamy 2020, Chhun *et al*. 2020, Chompoorat *et al*. 2019a, 2021).

The objective of this paper is to study the engineering properties with macro- and microscopic data of a lime- and cement-stabilised expansive clay obtained from the Mae Moh Power Plant. Lime-soil and cement-soil reactions were studied using mechanical tests and microstructural investigations. Mechanical tests included California bearing ratio (CBR), unconfined compression strength (UCS), resilient modulus (M_R), and free-free resonance (FFR) tests. An attempt was made to differentiate the extensively debated hydration and pozzolanic reactions to confirm and analyse each one's effects on the microstructure of clays; analyses included the use of scanning electron microscopy (SEM), x-ray diffraction (XRD), and energy dispersive spectroscopy (EDS), as well as measurement of macroscopic properties of the lime- and cement-blended expansive clays.

Table 1 Geotechnical index properties of the expansive clay used in this study

Property	Measured value
Silt content (%)	1
Clay content (%)	99
Liquid limit (%)	66
Plastic limit (%)	22
Plastic index (%)	44
Specific gravity	2.75
Optimum moisture content (%)	14.21
Maximum unit dry unit (kN/m^3)	18.05
Soil classification (USCS)	CH

Table 2 Summary of the chemical compositions of materials

Name of chemical	Symbol	Portion (wt.%) in the sample (%)		
		Expansive clay	Portland cement	Hydrated lime
Silicon dioxide	SiO_2	49.63	23.72	1.94
Aluminium oxide	Al_2O_3	19.14	4.28	-
Ferric oxide	Fe_2O_3	10.67	2.06	-
Calcium oxide	CaO	14.15	62.97	96.04
Magnesium oxide	MgO	1.37	1.85	1.57
Sodium oxide	Na_2O	0.24	0.64	0.04
Potassium oxide	K_2O	2.67	0.67	0.08
Phosphorous oxide	P_2O_5	0.10	0.12	0.12

2. Materials and methods

2.1 Materials

The expansive clay employed in this study was collected from a depth of 0.5-1.5 m below the ground surface from the Mae Moh Lignite Mine in Lampang province of northern Thailand. The geotechnical index properties of the expansive clay are summarized in Table 1. The clay's plasticity index of approximately 44% was considered high, and indicative of high-volume change potential for the soil.

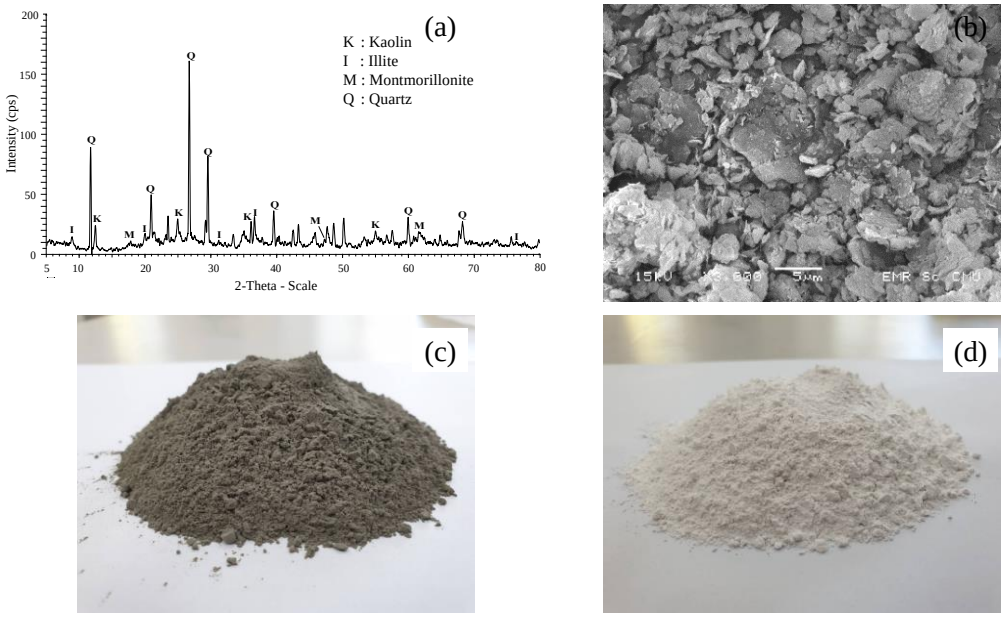

Fig. 1 (a) XRD pattern, (b) SEM image (3,000X magnification) of the expansive clay used in this study; (c) ordinary Portland cement type I and (d) hydrated lime used in this study

Table 3 Mixture proportion

Symbol	Cement (wt.%)	Lime (wt.%)
S (Untreated)	-	-
SC6	6	-
SC8	8	-
SC10	10	-
SC12	12	-
SL6	-	6
SL8	-	8
SL10	-	10
SL12	-	12

Table 4 Testing program

Test	Test sample	Curing time (d)	Sample condition
Free swelling	All samples	7	Soaked
CBR	S, SC10, SL10	7	Soaked and unsoaked
UCS	All samples	7, 28, 60, 90	Unsoaked
M_R	All samples	7, 28, 60, 90	Unsoaked
FFR	All samples	7, 28, 60, 90	Unsoaked
SEM	All samples	7, 28, 60, 90	Air-dried
XRD	S, SC6, SC10, SL6, SL10	7, 28, 60, 90	Air-dried
EDS	S, SC10, SL10	7, 28, 60, 90	Air-dried

Based on the unified soil classification system (USCS), this expansive clay was categorized as a CH. The chemical composition of the clay, as determined by x-ray fluorescence (XRF), is shown in Table 2. The expansive clay contained 49.63% silicon dioxide (SiO_2), 18.14% aluminium oxide (Al_2O_3), 8.49% ferric oxide (Fe_2O_3), 2.35% magnesium oxide (MgO), and 1.07% calcium oxide (CaO). The XRD analysis in Fig. 1(a) revealed that the major composition of the expansive clay was quartz (SiO_2) whereas montmorillonite, which is known as the most active clay mineral, was the major clay mineral. In addition, kaolinite and illite were also detected. Fig. 1(b) shows the SEM image of the untreated expansive clay before inundation. The particle size, shape and surface of each major components were definitely different. The SEM images showed evidence of randomly oriented flaky montmorillonite clay particles forming multi-particle aggregates of expansive clay.

Ordinary Portland cement (OPC) type I and hydrated lime were used as stabilisers in this study; their physical characteristics are presented in Figs. 1(c) and 1(d), respectively. The chemical composition data of the cement and lime obtained from XRF tests are shown in Table 2. Although the expansive clay contained a high SiO_2 content, their SiO_2 content is considered comparatively inert and unreactive to cement and lime. Both the cement and lime contained high CaO contents of 62.97% and 96.04%, respectively. CaO is the main chemical component involved in creating cementitious products; therefore, the selected cement and lime should be good candidates as clay stabilisers that can reduce the swelling potential and improve the strength and stiffness of the expansive clay for use as road material.

2.2 Method

2.2.1 Specimen preparation

The expansive clay was passed through a No. 40 sieve (0.425 mm) to remove coarse aggregates then dried for 24 h to make sure that its initial moisture content was zero before mixing with cement, lime, and water. Table 3 shows the mixture proportion of specimens. Engineering properties of the admixtures were determined in the laboratory; standard

methods were used to measure pH (ASTM 1999), free swelling test (ASTM 2003), CBR (ASTM 2016a), UCS (ASTM 2016b), and M_R of soil (AASHTO 2017). Dynamic modulus was measured from FFR tests according to the recommendation of ASTM C597 (ASTM 2016c). Considering the microstructure of each material, XRD, EDXRF, and SEM/EDS analyses were also performed. All test results are summarized in Table 4.

The optimum moisture content (OMC) and maximum dry unit weight ($\gamma_{d,max}$) of untreated and treated expansive clays with different amounts (wt.%) of cement and lime were determined by a series of compaction tests performed according to the modified Proctor test method in ASTM D 1557 (ASTM 2012). pH was measured for expansive clays with 0-18% of lime in accordance with ASTM D 6276 (ASTM 1999); special attention was given to control the room temperature at 25°C because the pH of lime-clay mixtures is temperature dependent. CBR tests were performed on clay with optimum lime content (OLC), which was 10% cement content and 10% lime content by soil dry weight (wt.% DW); tests were performed under unsoaked and soaked conditions with a curing period of 7 d.

Free swelling, UCS, M_R, and FFR tests was carried out on clays mixed with cement and lime contents of 6, 8, 10, and 12 wt.% DW. Predetermined OMCs were used as the water content for different cement and lime contents. A mixer was used to mix dry expansive clay, cement, lime, and water. Test samples were compacted to achieve the $\gamma_{d.max}$ of the modified Proctor test in a cylindrical mould 50 mm in diameter and 100 mm in high. The samples were forced out of the mould after 24 h, then cured for 7, 28, 60 and 90 days while wrapped in plastic sheets and stored in a foam box to avoid moisture loss.

2.2.2 pH test

The OLC is defined as the lowest percentage of lime required to keep a soil-lime-water solution at pH 12.4 or constant at 25°C (Bell 1996, Sharma *et al*. 2012). The simple Eads and Grim pH test (Eades and Grim 1966, ASTM 1999) was performed to identify the OLC of the clay. Clays with lime contents from 0-18 wt.% were evaluated. The OLC was found to be 10% lime by soil dry weight (wt.% DW) at pH 12.37. However, since this test does not provide reliable information on the potential reactivity of a particular expansive clay, or the magnitude of increased strength after its treatment at the OLC (Cherian and Arnepalli 2015), the percentage of lime or cement was varied between 6-12 wt.% DW for subsequent experiments in this study.

2.2.3 Free swelling test

Tests were conducted on expansive clays with different amount of cement and lime as summarized in Table 4. After 7 days curing, specimens with a diameter of 50 mm and a height of 100 mm were placed between two porous stones and then soaked by inundating it with water from both ends. No seating stress was applied during test. The vertical swell movements were recorded at different times through a dial gauge. Tests were stopped when swell movement ceased to be detected through the dial gauge readings for a period of 24 h. All tests were carried out at room temperature.

2.2.4 CBR test

CBR test samples measured 152 mm in diameter and 177 mm in height were cured for 7 days. Tests were performed under unsoaked and soaked conditions as shown in Table 4. For CBR tests performed under soaked conditions, test molds were immersed in water with a surcharge of 4.5 kg for 4 d. A Universal testing machine (UTM) with a capacity of 50 kN was used to test both soaked and unsoaked test specimens. A load rate of 1.27 mm/min was applied by the UTM's penetration plunger, and the resultant stress and displacement data were then plotted. To calculate CBR values, stress data was divided by reference stresses and multiplied by 100.

2.2.5 UCS test

UCS tests were carried out on clays with different cement and lime contents as summarized in Table 4. After curing, test specimens were placed in an automatic UTM with a capacity of 50 kN. Specimens were placed under strain at a rate of 1.0%/min until the specimen failed or 15% strain was reached, whichever occurred first. Triplicate tests conducted for specimens of each curing time.

2.2.6 M_R test

M_R test was performed using a dynamic UTM. A load duration format of 1:9 (0.1 s loading and 0.9 s rest periods) was applied to each specimen based on the haversine shape function. A seating stress at 10% of the deviator stress was also used during the loading duration. As samples changed with the state of stress, two linear variable deferential transducers (LVDT's) were used to measure the vertical permanent strain, while the loading cell measured the deviator stress. To account for changes to the samples as stress was applied, each individual test was operated in 15 sequences in which each sequence had a different confining and axial stress level (for more details see AASHTO (2017)). The tests were stopped when either specimen failure occurred or the vertical permanent strain of the specimen reached 5%.

2.2.7 FFR test

FFR assay was performed to determine the dynamic modulus of clay samples under a small strain. The testing method involved hanging a sample on a rigid frame in the horizontal direction and suspending it with a tendon to approach free boundary conditions. To measure vibrations, an accelerometer was set in contact with one end of the sample, while the other end was knocked with a light hammer. E_0 and G_0 values were calculated from Eqs. (1) and (2), respectively.

$$E_0 = \rho v_p^2 = \rho(2Lf_L)^2 \quad (1)$$

$$G_0 = \rho v_s^2 = \rho(2Lf_T)^2 \quad (2)$$

where ρ is the bulk density, L is the length of the specimen, f_L is the longitudinal resonant frequency, f_T is the torsional resonant frequency, v_p is the longitudinal (compressive) wave velocity, and v_s is the torsional (shear) wave velocity.

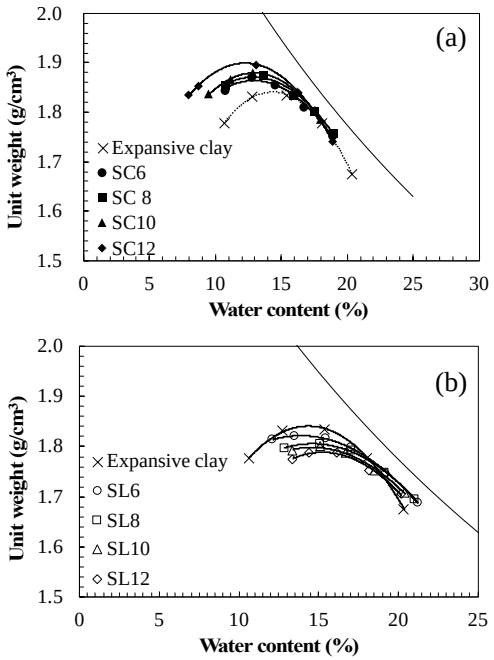

Fig. 2 Compaction curve of expansive clay admixed with 6, 8, 10 or 12 wt.% of (a) cement (SC) or (b) lime (SL)

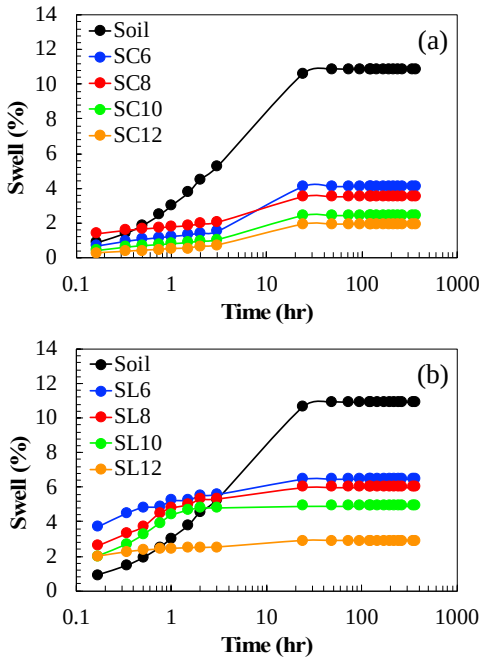

Fig. 3 Swelling versus time of expansive clay admixed with 6, 8, 10 or 12 wt.% of (a) cement (SC) and (b) lime (SL)

2.2.8 XRD test

XRD test was performed to determine the structure of crystalline materials in the expansive clay mixed with cement and lime. XRD analyses were carried out on small piece of samples obtained from selected specimen. The samples were freeze-dried and passed through a No. 200 (0.075 mm) sieve. Particles smaller than 0.075 mm were set on a sample holder for testing. XRD data were collected at every 0.02° between 2°-80°.

2.2.9 EDXRF and SEM/EDS tests

EDXRF and SEM/EDS were performed to identify microstructural changes in the expansive clay stabilised with cement and lime. Small pieces of sample were collected from the failure position of the UCS tests. Samples were selected to be approximately 5 mm long. Once collected, the samples were stored in a zip bag with desiccant to dry. Then, a selected dry sample would be coated with a thin layer of gold using a sputter-coater before being placed on a sample holder for the EDXRF and SEM/EDS tests.

3. Results and discussion

3.1 Compaction test

The compaction curves of untreated and treated expansive clay are illustrated in Fig. 2. The compaction curve of expansive clay was clearly dependent on cement content, as the expansive clays with 6, 8, 10 and 12 wt.% of cement all had significantly higher $\gamma_{d,max}$ and lower OMC than that of the pure expansive clay. For comparison, the un-stabilised expansive clay had a $\gamma_{d,max}$ of 1.84 g/cm^3 at an OMC of 14.21%, while the clay blend with cement had $\gamma_{d,max}$ values in the range of 1.87-1.89 g/cm^3 with OMCs between 12.33-13.44%. On the other hand, the expansive clays with 6, 8, 10 and 12 wt.% of lime expressed a decrease in $\gamma_{d,max}$ and a slightly higher OMC. The $\gamma_{d,max}$ values of the lime-treated expansive clay were between 1.80-1.82 g/cm^3 with OMC values between 13.50 and 15.15%. This is very similar to the result obtained from previous research (Bell 1996, Al-Taie *et al*. 2015) where the addition of lime affected the flocculation process into producing card-house type clay structures that resisted compaction and gave way to a lower density and higher moisture content as the lime-stabilised clay required more water for pozzolanic reactions to occur. Moreover, since lime is generally composed of CaO, lime particles are quite small compared with the expansive clay.

3.2 Free swelling test

Swelling behaviour can be separated into three stages (Azam and Wilson 2006): (1) A beginning low swelling stage due to low unsaturated hydraulic conductivity; (2) a main intermediate swelling stage related to a confirmed wetting front; and (3) a lesser, low swelling stage caused by near-saturation conditions. Fig. 3 displays the relation between swelling values and time for untreated and treated expansive clays with different cement and lime contents of 6, 8, 10 and 12 wt.%. As expected, expansive clay admixtures with cement exhibited three swelling stages: An initial swelling that increased slowly with time, then swelling which occurred more quickly, and finally practical cessation of swelling at a constant terminal value.

The untreated expansive clay, with had a maximum swelling of 10.9%, is unsuitable for road construction because its swelling value is higher than 9% (Seed *et al*.

Table 5 Summary of the different test results for the pure clay (S) and that admixed with different wt.% levels of cement (SC) and lime (SL)

Test	Condition	S	SC6	SC8	SC10	SC12	SL6	SL8	SL10	SL12
CBR (%)	Unsoaked	59.0 ± 0.6	-	-	198.8 ± 6.1	-	-	-	93.5 ± 5.1	-
	Soaked	3.8 ± 0.6	-	-	17.5 ± 1.0	-	-	-	11.4 ± 0.8	-
UCS (kPa)	7 d	680.0 ± 27.4	2,899.8 ± 113.8	3,229.0 ± 149.0	3,380.0 ± 160.0	3,837.4 ± 59.8	1,865.1 ± 130.4	2,049.8 ± 92.4	2,512.3 ± 162.3	2,013.5 ± 87.5
	28 d	-	3,446.5 ± 283.6	4,377.7 ± 327.2	5,372.9 ± 312.0	5,615.5 ± 218.4	3,563.0 ± 237.5	3,595.9 ± 302.4	3,111.7 ± 172.2	3,137.0 ± 311.7
	60 d	-	4,970.1 ± 27.8	6,026.3 ± 237.9	6,185.0 ± 286.0	6,475.9 ± 638.5	3,690.5 ± 85.0	4,492.3 ± 126.3	4,735.9 ± 70.4	3,984.2 ± 127.8
	90 d	-	6,013.5 ± 159.3	7,174.7 ± 156.0	7,289.3 ± 828.6	7,684.7 ±190.2	4,480.2 ± 169.2	4,410.9 ± 310.1	3,985.6 ± 110.8	3,900.0 ± 163.0
E_0 (MPa)	7 d	581.0 ± 28.9	3,178.0 ± 62.4	3,670.0 ± 99.7	4,850.8 ± 72.9	4,838.5 ± 183.7	1,661.8 ± 58.1	1,746.0 ± 20.8	2,022.9 ± 39.6	2,298.3 ± 72.2
	28 d	-	4,366.8 ± 157.8	4,820.1 ± 55.6	5,760.3 ± 57.4	6,378.0 ± 69.6	3,223.6 ± 30.2	3,599.4 ± 24.7	3,739.0 ± 15.9	3,395.6 ± 3 5.7
	60 d	-	4,788.5 ± 108.5	5,590.2 ± 87 .5	5,426.0 ± 157.9	6,148.2 ± 205.3	3,730.2 ± 16.6	2,992.0 ± 44.8	4,066.7 ± 28.9	3,112.1 ± 37.9
	90 d	-	5,107.8 ± 80.5	5,901.1 ±199.4	5,542.6 ± 140.3	6,915.5 ± 195.6	2,933.9 ± 46.3	2,851.9 ± 53.7	2,916.7 ± 88.2	2652.8 ± 79.0
M_R (MPa)	7 d	345.0 ± 35.2	848.5 ± 46.0	924.3 ± 52.3	975.9 ± 41.3	987.6 ± 3.8	873.3 ± 57.6	950.1 ± 44.2	777.3 ± 54.8	847.7 ± 56.2
	28 d	-	816.1 ± 4.0	959.0 ± 22.4	1,008.7 ± 26.0	931.7 ± 54.7	876.8 ± 34.4	852.8 ± 18.3	969.3 ± 26.6	902.6 ± 36.5
	60 d	-	1,028.2 ± 3.7	950.2 ± 7.1	912.1 ± 65.5	932.1 ± 45.1	933.5 ± 16.4	847.6 ± 17.3	921.6 ± 7.2	865.1 ± 43.2
	90 d	-	981.3 ± 11.4	917.5 ± 11.4	944.9 ± 10.9	969.2 ± 24.5	945.7 ± 19.5	938.3 ± 30.8	898.9 ± 35.7	736.0 ± 58.7
G_0 (MPa)	7 d	186.0 ± 24.8	1,232.8 ± 109.4	1,370.7 ± 35.4	1,821.1 ± 56.4	1,916.1 ± 25.0	1,133.5 ± 108.0	1,247.0 ± 58.0	1,274.5 ± 55.9	884.9 ± 18.8
	28 d	-	1,772.3 ± 102.1	1,840.0 ± 23.6	2,111.6 ± 28.2	2,336.9 ± 56.2	1,367.8 ± 27.0	1,335.7 ± 10.9	1,391.4 ± 49.5	1,407.7 ± 6.4
	60 d	-	1,854.8 ± 71.1	2,137.5 ± 289.7	2,054.3 ± 54.9	2,428.5 ± 119.5	1,363.3 ± 23.8	1,553.8 ± 10.2	1,611.3 ± 10.3	1,082.8 ± 192.9
	90 d	-	1,942.9 ± 52.3	2,131.1 ± 117.2	2,050.2 ± 117.2	2,480.8 ± 90.0	1,576.0 ± 28.2	1,497.7 ± 82.1	1,632.1 ± 22.4	1,572.2 ± 140.8

Note: Data are shown as the mean ± standard error (SE), derived from triplicate trials

1962, Puppala *et al*. 2004). However, when cement was used to treat the expansive clay, as in samples of SC6, SC8, SC10, and SC12, maximum swelling values were reduced to 4.11, 3.53, 2.42 and 1.93%, respectively. Likewise, when lime was used to treat the expansive clay, maximum swelling values were recorded as 6.5, 6.0, 5.0 and 3.0 % for SL6, SL8, SL10 and SL12, respectively. These results show that both cement and lime treatment will abate the swelling problems of pure expansive clay, making admixtures of clay and cement or lime suitable for use as road construction material.

SC12 showed over 8% of decrease in maximum swelling value over pure expansive clay, the most improvement of any cement-treated expansive clays. This was mainly the result of the hydration gels formed in the initial hydration reaction progressively crystallizing to build an interlocking clay structure. The cementation between clay minerals and cement slowly induces the substitution of sodium ions (Na^+) with calcium ions (Ca^{2+}) in montmorillonite. As for lime-treated clay, lime addition actually seemed to increase the initial swelling of the admixture, but the final maximum swelling values of the admixtures eventually exhibited 4.5-8% improvement over pure expansive clay. This improvement in swelling behavior was caused by the lime promoting pozzolanic reactions while the specimens were soaking in water.

3.3 Evaluation of the CBR

The CBR of the untreated expansive clay and the

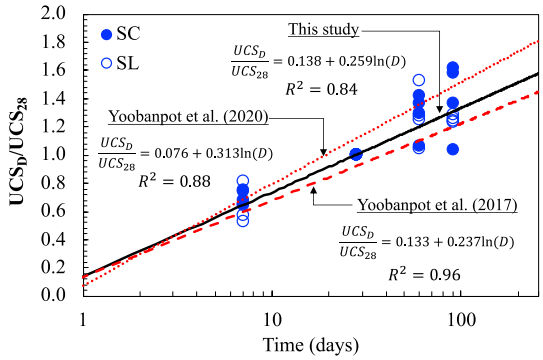

Fig. 4 Normalised UCS against time

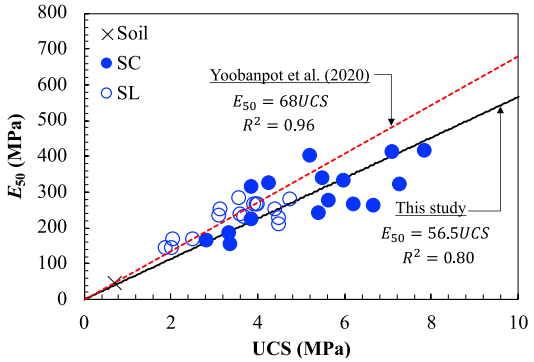

Fig. 5 Relationship between E_{50} and UCS

expansive clays admixed with cement or lime at 10 wt.% optimum level were evaluated in the laboratory; results are shown in Table 5. The CBR value of the pure expansive clay in unsoaked and soaked conditions were 59.0% and 3.8%, respectively. When the expansive clay was blended with 10 wt.% cement or lime and, after 7 days of curing, CBR of unsoaked samples were 198.76% and 93.50%, respectively, while CBR of soaked samples were 17.5 and 11.4%, respectively. The increase in CBR values after addition of these stabilisers was attributed to the hydration reaction after cement addition, which resulted in a reduced plasticity and strength gain, and the pozzolanic reaction between the soil's silica and alumina with lime, which formed various types of cementing agents.

3.4 UCS test

The UCS of samples were measured after 7, 28, 60 and 90 d curing. The base UCS of the untreated specimen was 680 kPa, while the UCS values of all treated specimens increased regardless of curing time, as present in Table 5. In expansive clay samples treated with cement, the UCS values clearly increased in the first 28 d. This UCS increase was due to the cement's hydration process taking up and decreasing the mixtures' water content, causing the cement-treated clay to harden. Furthermore, additional curing time allowed the cement-clay admixtures to harden further, providing further UCS improvements. UCS was also expected to rise in accordance with increased cement content (Chompoorat and Likitlersuang 2016, Julphunthong *et al.* 2018, Chompoorat *et al.* 2019a); therefore, as expected, the increases in UCS were larger as cement content increased in this study as well.

The UCS of expansive clay stabilised with different wt.% of lime after different curing periods are also shown in Table 5. The shear strength of specimens continually increased with curing time; for example, the UCS of specimens with 6 wt.% lime content increased from 1865 kPa after 7 d of curing, to 4480 kPa after 90 d. When comparing admixtures with different lime contents, the UCS of specimens with 6, 8, 10 and 12 wt.% lime content after 28 days of curing were 3563, 3595, 3111 and 3136 kPa, respectively. As such, it was concluded that, although all specimens with lime displayed UCS improvements over pure expansive clay, the added benefit starts to decline at beyond 10 wt.% lime content; in other words, 10 wt.% lime was the OLC according to this study's results. The loss in strength at higher lime contents may be due to the fact that lime itself does not have either appreciable friction or cohesion. As a result, a high lime content would serve as a lubricant in between soil particles, leading to reduced strength. It should also be noted that long-term reactions between lime and sulphate-rich soils can lead to the generation of secondary minerals, such as ettringite (Et) and thaumasite; crystallization of these materials may cause expansion of the treated soils over longer periods of time (Bell 1996, Nicholson 2015).

The gradual development of UCS in the cement- and lime- admixed expansive clays were normalised by the UCS at 28-days of curing (UCS_{28}), as suggested by Horpibulsuk *et al.* (2011, 2012). Normalised values expressed a linear correlation on a semi-log plot, with a correlation coefficient (R^2) of 0.84. The normalised correlation found in this study was quite close to correlations found in previously studies, specifically studies on dredged sediments stabilised with cement and fly ash (Yoobanpot *et al.* 2020), and soft clay stabilised with cement kiln dust and fly ash residue (Yoobanpot *et al.* 2017) as shown in Fig. 4. It is noted that UCS increases over time should be similar in samples made up of the same soil type because the development of soil strength is essentially controlled by the degree of chemical reactions.

Similar to UCS values, the secant Young's modulus at 50% strength (E_{50}) determined by UC tests also increased with curing period. The ratios between the stiffness and strength (E_{50}/UCS) were rather constant for both cement- and lime- improved clays as illustrated in Fig. 5. The E_{50}/UCS ratios of this study were 56.5 with an R^2 value of 0.80, which is consistent with the findings of past studies (Yoobanpot *et al.* 2020), with small differences being ascribed to different clay minerals and water-per-binder ratio used.

3.5 M_R test

M_R tests were performed based on the M_R protocol of the AASHTO T307 (AASHTO 2017) standard for unbound material. Table 5 shows the mean value of resilient modulus after 15 cycles for both the control (untreated) specimen and the 6-12 wt.% cement-admixed expansive clay specimens after 7, 28, 60 and 90 d of curing. The average M_R achieved for the control was 340 MPa, with cement

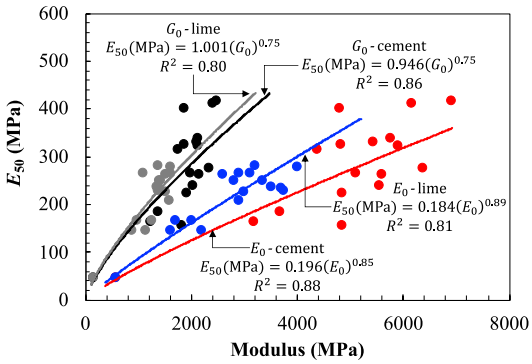

Fig. 6 Relationship between E_0, G_0 and UCS

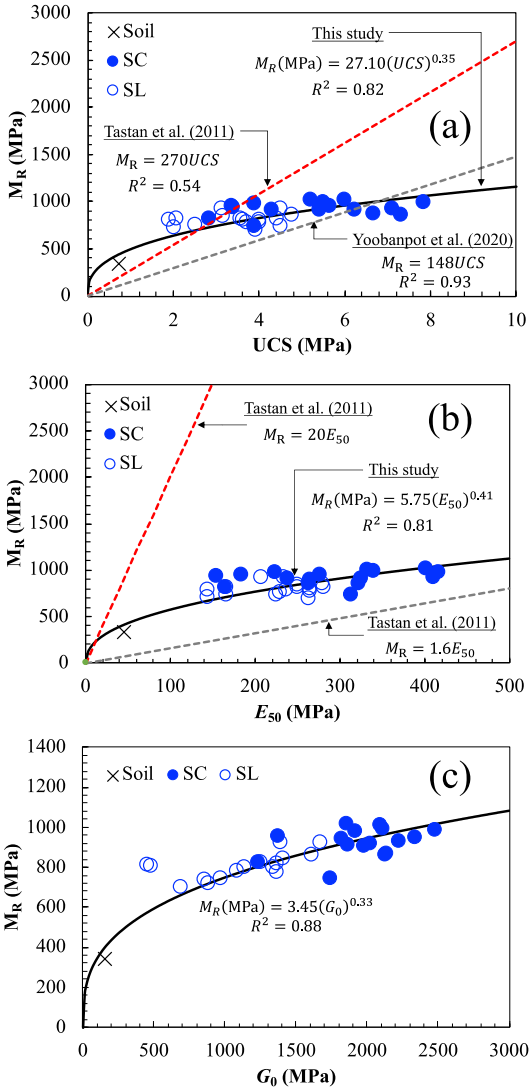

Fig. 7 (a) Relationship between M_R and UCS, (b) relationship between M_R and E_{50} and (c) relationship between M_R and v_s

treatment increasing sample M_R values by approximately 35-45%, and lime treatment increasing M_R values by approximately 40-45%, both compared to the control. Neither the resilient moduli of soil- or lime-cement mixes showed clear dependence on curing time (Chompoorat *et al.* 2018).

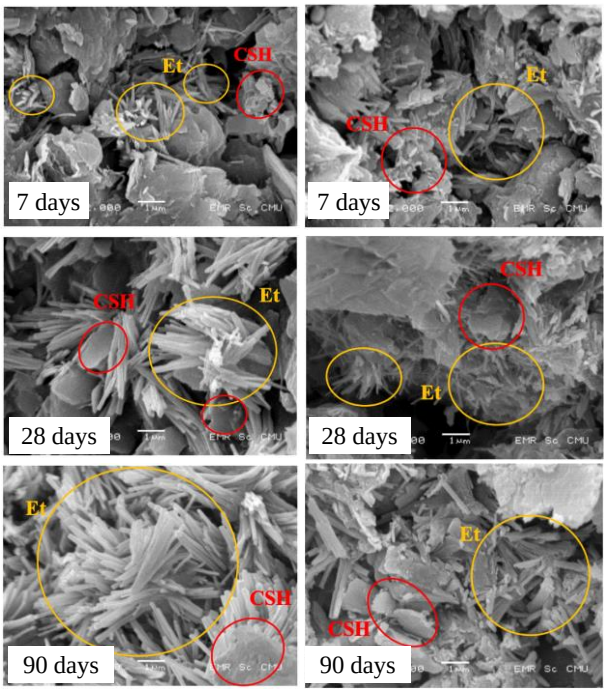

(a) (b)

Fig. 8 Representative SEM images (12,000X magnification) of the expansive clay admixed with cement after curing for (a) 6 wt.% and (b) 10 wt.%

3.6 FFR test

The FFR test was performed to observe the processes of the hydration and pozzolanic reactions that caused strength increase through microstructure formation. An observable increase in wave velocity over time through the FFR test would imply an increased stiffness owing to the hydration and pozzolanic reactions (Chompoorat *et al.* 2019b).

E_0 and G_0 values were calculated from measured values of v_p and v_s using Eqs. (1) and (2), respectively; results are displayed in Table 5 for each mixture after different curing periods. The increased dynamic modulus, which corresponded to the increased resonance wave velocity, indicated that cement had initially set after 7 d of curing. As anticipated, the calculated small-strain stiffness moduli increased with curing time due to cement hydration. The order of magnitude and increasing rate of the evaluated moduli agree well with results previously published in literature on cement-stabilised soft clay (e.g., Verástegui-Flores *et al.* 2010, Fatahi *et al.* 2013). Amongst all mixtures after 7 d of curing, the E_0 and G_0 values of mix SC12 (12 wt.% cement) was the highest, while mix SC6 (6 wt.% cement) had the lowest values.

E_0 and G_0 values versus curing time for five different wt.% of clay-lime mixes are also shown in Table 5. For pure expandable clay (0 wt.% lime), the E_0 and G_0 values did not change significantly between different curing periods, indicating no effect based on curing period. The expansive clay without lime also had the lowest E_0 and G_0 values. However, once lime was added to form clay-lime mixtures, there was considerable variation in E_0 and G_0 values dependent on lime content, indicating a strong influence of

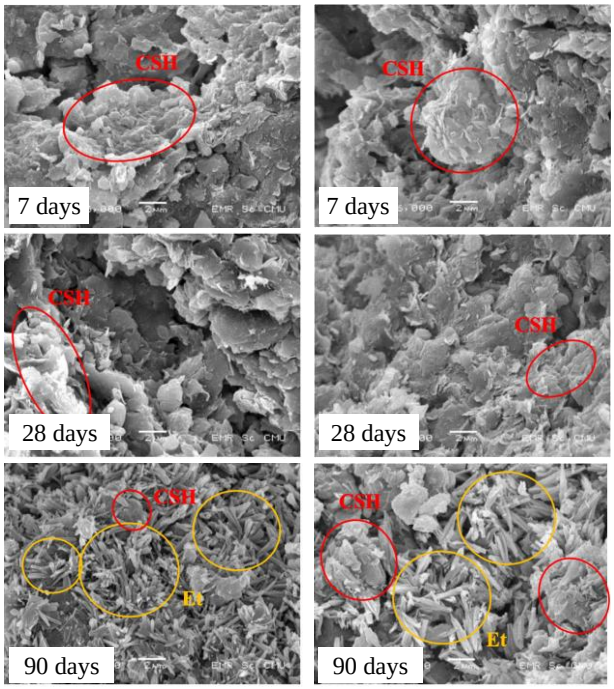

(a) (b)

Fig. 9 Representative SEM images (6,000X magnification) of the expansive clay admixed with lime after curing for (a) 6 wt.% and (b) 10 wt.%

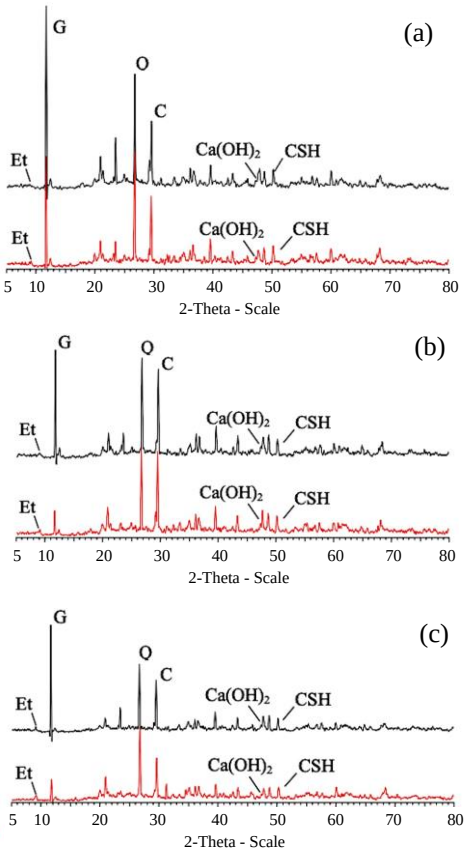

Fig. 10 XRD patterns for the expansive clay admixed at 6 wt.% (black) and 10 wt.% (red) cement after being cured for (a) 7 d, (b) 28 d and (c) 90 d

lime content on E_0 and G_0. At 7, 28 and 60 d of curing, the clay with 10 wt.% lime showed the highest values of E_0 and G_0 (consistent with the OLC). These results show that deviating from the OLC of 10 wt.%, whether decreasing or increasing lime content to 8 or 12 wt.%, E_0 and G_0 values will decrease. It was also observed that after 90 d of curing, 6 wt.% lime clay showed the highest E_0 and G_0 values. This may be indicative of long-term reactions between the lime and the soil's sulphate content, which can lead to the generation of secondary minerals such as Et and thaumasite; the crystallization of these secondary minerals may cause cracking of the treated soils over longer periods of time.

Fig. 6 illustrates the relationship between E_0 obtained from UC tests, and E_0 and G_0 values obtained from FFR tests. There is a clear trend of E_{50}, E_0, and G_0 values all increasing as the amount of cement or lime in the clay mixtures increase. As pore fluids in the cement- and lime-improved expansive clays changed, they were expected to influence vs, and consequently G_0 as well. Likewise, as the skeleton stiffness of the improved expansive clays developed after 28-days of curing, v_p and E_0 were also expected to raise. Therefore, it can be concluded that cement and lime content both play significant roles in the increment of E_{50}, E_0 and G_0.

3.7 Strength and stiffness correlations

This section presents the correlations of this experiment's quantitative results. The resilient moduli (M_R) were plotted against UCS, as shown in Fig. 7(a). It was found that M_R nonlinearly increased with UCS for both cement- and lime- stabilised expansive clays. The empirical equation between M_R and UCS was well fitted by a power function as shown in Fig. 7(a), which is different to the linear functions found in previous studies involving organic soil treated with fly ash (Tastan *et al*. 2011) and dredged sediments stabilised with cement and fly ash (Yoobanpot *et al*. 2020). The relationship between M_R and E_{50} was fitted well by a power function with an R^2 value of 0.81, as shown in Fig. 7(b). M_R versus E_{50} data points laid within the data range of a previous study involving organic soils admixed with fly ash (Tastan *et al*. 2011). Fig. 7(c) shows the relationship between M_R and G_0 from FFR tests, which fitted well to a power function with an R^2 value of 0.88. In general, the M_R value increased with G_0 as the latter ranged within 500-2,500 MPa.

3.8 Microstructure

Since changes in the macro-properties of the clay are fundamentally controlled by microstructural changes, SEM images of the expansive clay admixtures were captured to analyse these microstructure changes. Fig. 8 shows representative SEM images of the expansive clay admixed with different amounts of cement after curing for 7, 28 and 90 d. After 7-d of curing, the original structure of the expansive clay had already completely changed. In Fig. 1(b), it can be seen that flake-shaped particles had almost disappeared, and the structure was denser with particles connected to each other more strongly; this represents the

Table 6 Effect of cement- and lime-stabilisation on the CSH and Et intensities of expansive clay

Stabiliser	Content (wt.%)	Curing (d)	CSH intensity (%)	Et intensity (%)
Cement	6	7	0.09	0.04
		28	0.60	0.07
		60	1.46	1.35
		90	7.14	3.15
	10	7	3.81	0.34
		28	7.29	1.05
		60	8.91	3.53
		90	9.96	4.48
Lime	6	7	0.11	0.02
		28	1.05	0.08
		60	2.32	0.59
		90	7.41	2.93
	10	7	5.26	0.42
		28	5.58	1.13
		60	6.64	1.87
		90	8.90	2.46

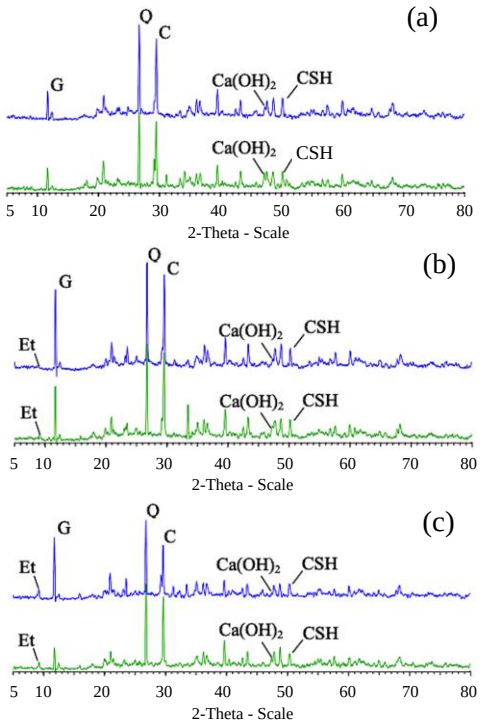

Fig. 11 XRD patterns for the expansive clay admixed at 6 wt.% (blue) and 10 wt.% (green) lime after being cured for (a) 7 d; (b) 28 d and (c) 90 d

hardening phase of the cement hydration products and involves the formation of Et crystals and CSH. As hydration products connected to one another, they formed a network to support any load acting on the stabilised clay, increasing the strength of the clay admixture as reflected by the UC and M_R test data obtained in this study. After 28 d of curing, solid structures were observable in the cement-admixed expansive clays, while the hydration products (Et and CSH) continued to solidify. After 90 d of curing, many rod-shaped hydration products had formed and protruded out from the cement particles (Fig. 9). The plate-shaped particles of CSH were also observed. Et crystals and CSH formations had inserted between clay particles and bonded to one another to form a large cluster; this reduced the pore size as formerly empty spaces were now occupied by new, mature crystal products of cement hydration (Horpibulsuk *et al*. 2010, Jamsawang *et al*. 2017, Chompoorat *et al*. 2019a, 2021).

Comparing admixtures with different cement content, as the relative amount of cement increased, the amount of cementitious hydration products that were observable in the pore spaces increased. Cementitious products not only improved the inter-cluster bonding strength, but also filled pore spaces. Thus, pore volume was significantly reduced with increasing cement content while shear strength increased.

SEM images of expansive clay stabilised with different amounts of lime and cured for different amounts of time are shown in Fig. 9. The microstructures of the 6 wt.% and 10 wt.% lime admixed clays showed the formation of smaller clusters of clay particles after 7 d of curing. The formation of these clusters was brought about by the pozzolanic activity initiated at the borders of the clay particles. After curing for 28 d, larger clusters were evident, as was the hardening of pozzolanic products (Et and CSH) which contributed to the improved strength of the clay. After 90 d of curing, there was still a larger increase in the size of the clay-lime clusters. It should be noted that the pozzolanic products increased and expanded from the lime grains to connect and surround the clay particles and form a strong bond between them.

SEM images taken at 6,000X magnification were used to analyse the soil-lime clusters formed. An increase in the size of clusters with increasing curing time served as evidence of particle aggregation and the formation of cementitious compounds taking place. In addition, after 90 d of curing, the samples depicted foil-like leafy structures with cemented clusters, which may be the intermediary formation of gel of the cementitious compounds. The SEM images distinctly showed the bonding filaments of the lime soil mixes. Previous studies by Arabi and Wild (1986), and Al-Rawas and McGown (1999) revealed a gradual breakdown of the clay particles and the formation of small to large interconnected aggregations, connectors and pore spaces. Although distinct clusters could not be found in our SEM images, an overall cemented morphology could be seen with higher proportions of lime. At 10 wt.% lime content, large interconnecting clusters were observed forming a composite material. This showed that the amount of transformation from a stacked structure to a leafy aggregated structure increased with higher lime content and longer curing times. This corresponds to the decreased strength observed in the UC, M_R, and FFR tests data.

Fig. 10 shows the XRD profiles of the un-stabilised expansive clay and clays stabilised by 6 and 10 wt.% of cement. XRD profiles can qualitatively indicate the level of

mineralogy in samples by comparing the intensity of sample signals with those of a reference powder. Several signal peaks for the cement-admixed expansive clays confirmed the formation of CSH, calcium hydroxide ($Ca(OH)_2$) and Et (Fig. 10), while the nonexistence of those peaks in the un-stabilised clay (Fig. 1(a)) showed that these formations did not occur in the pure clay, and that cement stabilisation was indeed related to hydration reactions. There was also a correlation between the diffraction intensities of CSH and Et with increasing cement contents. Furthermore, the intensities of these XRD signal peaks increased with curing time. The diffraction intensities of Et and CSH increased most markedly during the first two weeks of curing time, then increased more gradually before becoming almost constant for the long term (Fig. 10 and Table 6). Combining XRD and physical property test results, the amounts of CSH and Et that formed increased proportionally with UCS, M_R, and modulus. Thus, it could be concluded that these reaction products importantly contributed to the development of shear strength for the cement-treated clays.

Likewise, representative XRD profiles of the expansive clay stabilised with 6 and 10 wt.% lime after 7, 28, 60 and 90 d of curing are shown in Fig. 11. Compared with the un-stabilised clay (Fig. 1(a)), the lime-stabilised clay showed many more XRD signal peaks of low to moderate intensity, indicating the formation of new compounds. Among these, the major cementitious compounds were CSH, $Ca(OH)_2$, and Et, where stabilisation occurred due to the pozzolanic reaction. In the pozzolanic reaction, the calcium from lime reacts with soluble alumina and silica from clay in the presence of water to produce stable CSH, which creates long-term strength. The formation of Et is a result of the formation of CSH, which was a new pozzolanic compound in the lime-treated expansive clays. The visual reduction of XRD peaks at higher lime contents indicated the decay of the crystalline structure and formation of relatively amorphous compounds. At 6 and 10 wt.% lime content, the micrograph showed clear evidence of thorough CSH and Et development in a reticulated and flocculated form that allowed the clay to support a higher load (Table 6). Unfortunately, further increasing the lime content and curing time led to the formation of patches of reaction products that diminished the crystalline structure and developed strength.

Table 6 show the EDS results of the soil admixed with 10 wt.% cement and lime, respectively. The results showed that calcium (Ca), silica (Si), and aluminium (Al) were present in all specimens. The Ca content in both cement- and lime-stabilised expansive clay allowed for the formation of CSH gel that increased with an increasing curing period. At the same time, increasing the curing period tended to reduce the silicon and aluminium contents, but residual levels clearly remained. In conclusion, the shear strength of the expansive clay blended with cement or lime was mostly related to the amount of Ca. Additionally, the Si/Al ratio is important for building the bond strength of treated specimens. An increase in the Si/Al ratio helps to buffer the Ca content, helping treated samples develop greater shear strength through the increased creation of CSH gels and their associated bond strength (Bilondi *et al.* 2018). Therefore, the parameters affecting the shear strength of the stabilised samples are Ca content and the Si/Al ratio. Table 7 presents gel phase compositions of expansive clay stabilised with 10 wt.% admixtures. The Ca content and Si/Al ratio of the expansive clay admixed with 10 wt.% cement after curing for 7 d were 13.43% and 2.35%; these parameters increased at 28 d to 13.84% and 2.52% because of hydration reactions. On the other hand, the Ca content of the expansive clay admixed with 10 wt.% lime after 28 d of curing was 14.30%; this content slightly decreased after 60 d to 20.44% due to pozzolanic reactions. The Si/Al ratio of the expansive clay with 10 wt.% lime content after 7 d of curing was 2.2%, which increased with curing time to 2.27% at 28 d and 2.43% at 60 d.

Table 7 Gel phase compositions

Stabiliser	Content (wt.%)	Curing (d)	Ca (wt%)	Si (wt%)	Al (wt%)	Si/Al
Cement	10	7	13.43	21.83	9.29	2.35
		60	13.84	18.73	7.43	2.52
		90	21.58	14.64	6.30	1.47
Lime	10	7	14.30	15.51	7.06	2.20
		60	13.13	23.72	10.44	2.27
		90	19.00	10.63	8.21	1.29

4. Application of treated expansive clay as pavement materials

In its natural form, the Mae Moh expansive clay experiences swelling higher than 9%, making it necessary to mitigate the clay's swelling potential before it can be used as road material. It is also unsuitable as a subgrade layer due to its CBR value being lower than 5%. According to the Thailand Department of Highway's standard, after 7 days of curing, the required swelling value of clay should be lower than 4%, and the UCS of soil-cement bases and subbases should be higher than 1,724 and 689 kPa, respectively. Fig. 12 summarizes the property requirements (i.e., swelling, CBR, UCS and M_R values) for pavement materials according to the Thailand Department of Highway's standard. Comparing the results of this study with the requirements listed in Fig. 12, it is observed that the mixture of SC10 satisfies the requirements for both soil cement base and soil cement subbase. Furthermore, Austroads (2017) provides guideline values of M_R for unbound materials beneath a thin bituminous layer. The required M_R values for high standard crushed rock base course, normal standard crushed rock base course, base quality gravel, and subbase quality materials are 500, 350, 300 and 250 MPa, respectively. The results of this study show that the untreated expansive clay is appropriate for use as base quality gravel and subbase quality material; however, the cement- and lime- stabilised expansive clay will be required for use as high standard crushed rock base course and normal standard crushed rock base course, as shown in Fig. 12(d).

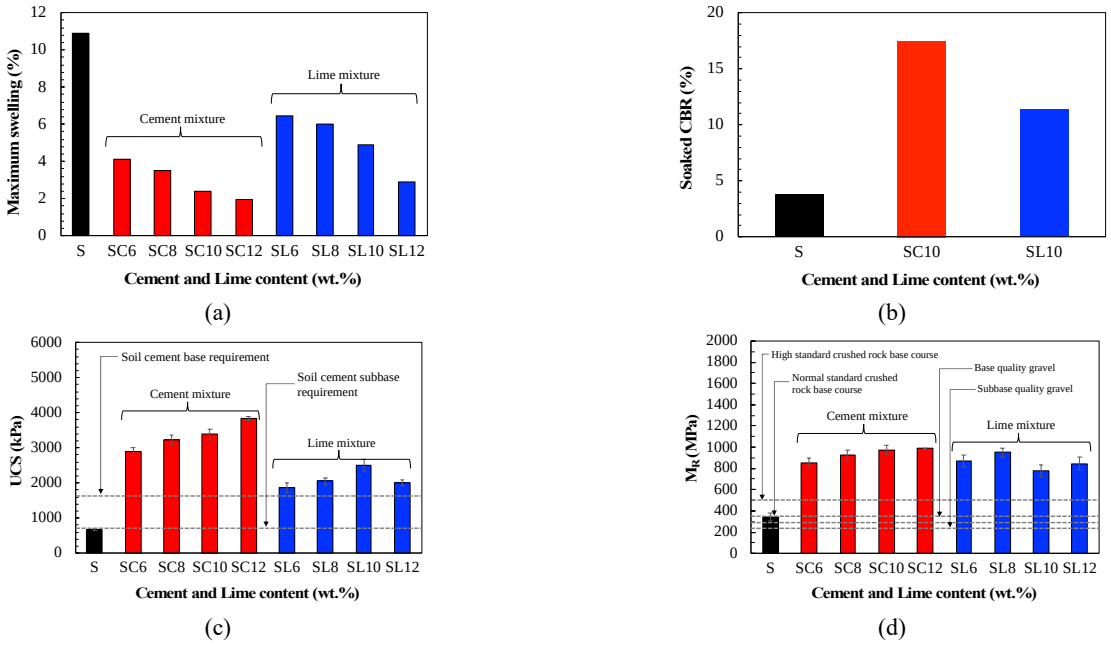

Fig. 12 Expansive clay admixed with different amounts (wt.%) of cement (SC) and lime (SL) at 7 days curing: (a) Maximum swelling, (b) CBR, (c) UCS and (d) M_R

5. Conclusions

The stabilisation of expansive clay with cement or lime was studied and the effects of the stabilisation on the mechanical and microstructural behaviour of the expansive clay were investigated.

• An improvement in the mechanical properties of the expansive clay was obtained by treatment with different wt.% of cement and different curing times. The treatment with cement increased the CBR, UCS, M_R and wave velocity, as well as the dynamic modulus of the clay. The magnitude of improvements aligned with increasing cement content and curing time.

• The OLC of a soil plays an important role in the progression of lime reactions. The OLC of the studied clay was found to be 10 wt.% through the Eades and Grim pH test. Less lime content than the OLC could not invoke permanent reactions due to an insufficient quantity of lime. Sufficient lime content, at the OLC or higher, can bring about pozzolanic reactions, which are more permanent and cause an increased strength and modulus. However, additional lime above the OLC reduces the overall strength gained due to the long-term reactions of the lime with the soil's sulphate content which lead to the generation of secondary minerals, such as ettringite (Et) and thaumasite. Crystallization of the secondary minerals lead to expansion, cracking, strength loss, and disintegration of the lime-treated expansive clay.

• SEM analysis supports the above conclusions and depicts more abundant formation of particle clusters with increasing curing time. A gradual breakdown of clay particles, as well as the formation of small to large interconnected aggregations, connectors, and pore spaces are characteristics of the microfabrics of cement- and lime-treated soils. A transformation from a stacked structure to a leafy-aggregated structure occurs with higher lime contents and longer curing times, which coincides with decreased strength of the admixed clay.

• XRD patterns show the formation of CSH, $Ca(OH)_2$, and Et in expansive clay stabilised with 6 and 10 wt.% cement or lime, with the CSH peak being predominant.

• Correlations between engineering properties and design parameters such as UCS, E_{50} and M_R can be suggested based on the comprehensive experimental results.

• It should be noted that based on the recommendation of Thailand's Department of Highways, the CBR, UCS and swelling values should meet the requirements for cement-treated base and subbase. In this study, both lime and cement stabilised dredged expansive soil met the CBR and UCS requirements, but only SC10 and SC12 satisfy the requirement of swelling. Therefore, the SC10 is highly recommended to use as base and subbase materials.

Data availability

All data, models and code generated or used during the study appear in the submitted article.

Acknowledgments

This research was supported by the National Research Council of Thailand (NRCT): NRCT5-RSA63001-05 and the Ratchadapisek Sompoch Endowment Fund (2020), Chulalongkorn University (763014 Climate Change and Disaster Management Cluster). The first author (T. Chompoorat) acknowledges the annual government statement of expenditure fund from the University of Phayao. The third author (S. Sitthiawiruth) acknowledges

the 60/40 Support for Tuition Fee from Chulalongkorn University. The fourth author (V. Komolvilas) acknowledges Grants for Development of New Faculty Staff, the Ratchadaphiseksomphot Endowment Fund, Chulalongkorn University, Thailand. The fifth author (P. Jamsawang) acknowledges the King Mongkut's University of Technology North Bangkok (KMUTNB) under Contract No. KMUTNB-62-KNOW-14. The last author (P. Jongpradist) acknowledges the King Mongkut's university of Technology Thonburi through Research Strengthening Project of the Faculty of Engineering. Special thanks to the Mae Moh mine's staff and the Chememan Public Company Limited for providing materials for this study.

References

AASHTO (2017), "Standard method of test for determining the resilient modulus of soils and aggregate materials", American Association of State Highway and Transportation Officials (AASHTO), Washington, D.C., U.S.A.

Al-Bared, M.A., Harahap, I.S., Marto, A., Mohamad, H., Abad, S.V.A.N.K. and Mustaffa, Z. (2020), "Cyclic behavior of RT-cement treated marine clay subjected to low and high loading frequencies", *Geomech. Eng.*, **21**(5), 433-445. http://doi.org/10.12989/gae.2020.21.5.433.

Al-Mukhtar, M., Khattab, S. and Alcover, J. (2012), "Microstructure and geotechnical properties of lime-treated expansive clayey soil Muzahim", *Eng. Geol.*, **139-140**, 17-27. https://doi.org/10.1016/j.enggeo.2012.04.004.

Al-Rawas, A.A. and McGown, A. (1999), "Microstructure of Omani expansive soils", *Can. Geotech. J.*, **36**(2), 272-290. https://doi.org/10.1139/t98-111.

Alrubaye, A.J., Hasan, M. and Fattah, M.Y. (2018), "Effects of using silica fume and lime in the treatment of kaolin soft clay", *Geomech. Eng.*, **14**(3), 247-255. http://doi.org/10.12989/gae.2018.14.3.247.

Al-Taie, A.Y., Disfani, M.M., Evans, R.P., Arulrajah, A. and Horpibulsuk, S. (2015), "Determination of optimum lime content for volcanic expansive clays", *Fund. Appl. Geotech.*, 1623-1630. https://doi.org/10.3233/978-1-61499-603-3-1623.

Arabi, M. and Wild, S. (1986), "Microstructural development in cured soil-lime composites", *J. Mater. Sci.*, **21**(2), 497-503. https://doi.org/10.1007/BF01145514.

ASTM (1999), Standard test method for using pH to estimate the soil-lime proportion requirement for soil stabilization, ASTM D6276, ASTM International, Philadelphia, U.S.A.

ASTM (2003), Standard test methods for one-dimensional swell or swell settlement potential of cohesive soils, ASTM D4546, ASTM International, Philadelphia, U.S.A.

ASTM (2012), Standard test methods for laboratory compaction characteristics of soil using modified effort (56,000 ft-lbf/ft3 (2700 kN-m/m^3)), ASTM D 1557, ASTM International, Philadelphia, U.S.A.

ASTM (2016a), Standard test method for California bearing ratio (CBR) of laboratory-compacted soils, ASTM D 1883, ASTM International, Philadelphia, U.S.A.

ASTM (2016b), Standard test method for unconfined compressive strength of cohesive soil, ASTM D 2166/D 2166M, ASTM International, Philadelphia, U.S.A.

ASTM (2016c), Standard test method for pulse velocity through concrete, ASTM C597-16, ASTM International, Philadelphia, U.S.A.

Austroads (2017), *Guide to Pavement Technology Part 2: Pavement Structural Design*, Austroads, Sydney, Australia.

Avsar, E., Ulusay, R. and Sonmez, H. (2009), "Assessments of swelling anisotropy of Ankara clay", *Eng. Geol.*, **105**(1-2), 24-31. https://doi.org/10.1016/j.enggeo.2008.12.012.

Azam, S. and Wilson, G.W. (2006), "Volume change behavior of a fissured expansive clay containing anhydrous calcium sulfate", *Proceedings of the 4th International Conference on Unsaturated Soils*, Carefree, Arizona, U.S.A., April.

Bell, F.G. (1996) "Lime stabilization of clay minerals and soils", *Eng. Geol.*, **42**(4), 223-237. https://doi.org/10.1016/0013-7952(96)00028-2.

Bilondi, M.P., Toufigh, M.M. and Toufigh, V. (2018), "Experimental investigation of using a recycled glass powder-based geopolymer to improve the mechanical behavior of clay soils", *Constr. Build. Mater.*, **170**, 302-313. https://doi.org/10.1016/j.conbuildmat.2018.03.049.

Boardman, D.I., Glendinning, S. and Rogers, C.D.F. (2001), "Development of stabilization and solidification in lime-clay mixes", *Geotechnique*, **51**(6), 533-543. https://doi.org/10.1680/geot.2001.51.6.533.

Bozbey, I., Kelesoglu, M.K., Oztoprak, S., Komut, M., Comez, S., Ozturk, T., Mert, A. and Ocal, K. (2021), "Effects of soaking on a lime stabilized clay and implications for pavement design", *Geomech. Eng.*, **24**(2), 115-127. http://doi.org/10.12989/gae.2021.24.2.115.

Brandl, H. (1981), "Alteration of soil parameters by stabilization with lime", *Proceedings of the 10th International Conference on Soil Mechanics and Foundation Engineering*, Stockholm, Sweden, June.

Cherian, C. and Arnepalli, D.N. (2015), "A critical appraisal of the role of clay mineralogy in lime stabilization", *Int. J. Geosynth. Ground Eng.*, **1**(8), 1-20. https://doi.org/10.1007/s40891-015-0009-3.

Chhun, K.T., Choo, H., Kaothon, P. and Yune, C.Y. (2020), "Experimental study on the strength behavior of cement-stabilized sand with recovered carbon black", *Geomech. Eng.*, **23**(1), 31-38. http://doi.org/10.12989/gae.2020.23.1.031.

Chompoorat, T. and Likitlersuang, S. (2016), "Assessment of shrinkage characteristic in blended cement and fly ash admixed soft clay", *Proceedings of the 15th Asian Regional Conference on Soil Mechanics and Geotechnical Engineering*, Kyushu, Japan, November. https://doi.org/10.3208/jgssp.THA-01.

Chompoorat, T., Likitlersuang, S. and Jongvivatsakul, P. (2018), "The performance of controlled low-strength material base supporting a high-volume asphalt pavement", *KSCE J. Civ. Eng.*, **22**(6), 2055-2063. https://doi.org/10.1007/s12205-018-1527-z.

Chompoorat, T., Maikhun, T. and Likitlersuang, S. (2019a), "Cement improved lake bed sedimentary soil for road construction", *Proc. Inst. Civ. Eng. Ground Improv.*, **172**(3), 192-201. https://doi.org/10.1680/jgrim.18.00076.

Chompoorat, T., Likitlersuang, S. and Jongvivatsakul, P. (2019b), "Engineering properties of controlled low-strength material (CLSM) as an alternative fill material", *Proceedings of the 16th Asian Regional Conference on Soil Mechanics and Geotechnical Engineering (16ARC)*, Taipei, Taiwan, October.

Chompoorat, T., Thanawong, K. and Likitlersuang, S. (2021), "Swell-shrink behaviour of cement with fly ash-stabilised lakebed sediment", *B. Eng. Geol. Environ.*, **80**, 2617-2628. https://doi.org/10.1007/s10064-020-02069-2.

Croft, J.B. (1967), "The influence of soil mineralogical composition on cement stabilization", *Geotechnique*, **17**(2), 119-135. https://doi.org/10.1680/geot.1967.17.2.119.

Diamond, S. and Kinter, E.B. (1965), "Mechanisms of soil-lime stabilization", *Highway Res. Rec.*, **92**, 83-102.

Eades, J.L. and Grim, R.E. (1966), "A quick test to determine lime requirements for lime stabilization", *Highway Res. Rec.*, **139**,

61-72.
Fatahi, B., Fatahi, B., Le, T.M. and Khabbaz, H. (2013), "Small-strain properties of soft clay treated with fibre and cement", *Geosynth. Int.*, **20**(4), 286-300. https://doi.org/10.1680/gein.13.00018.
Freitas, J.B., Rezende, L.R. and Gitirana Jr., G.F.N. (2020), "Prediction of the resilient modulus of two tropical subgrade soils considering unsaturated conditions", *Eng. Geol.*, **270**, 5. https://doi.org/10.1016/j.enggeo.2020.105580.
Ghiyas, S.M.R. and Bagheripour, M.H. (2020), "Stabilization of oily contaminated clay soils using new materials: Micro and macro structural investigation", *Geomech. Eng.*, **20**(3), 207-220. http://doi.org/10.12989/gae.2020.20.3.207.
Ghose, A. and Subbarao, C. (2007), "Strength characteristics of class F fly ash modified with lime and gypsum", *J. Geotech. Geoenviron. Eng.*, **133**(7), 757-766. https://doi.org/10.1061/(ASCE)1090-0241(2007)133:7(757).
Guidobaldia, G., Cambi, C., Cecconi, M., Deneele, D., Paris, M., Russo, G. and Vitale, E. (2017), "Multi-scale analysis of the mechanical improvement induced by lime addition on a pyroclastic soil", *Eng. Geol.*, **221**, 193-201. https://doi.org/10.1016/j.enggeo.2017.03.012.
Horpibulsuk, S., Rachan, R., Raksachon, Y., Suddepong, A. and Chinkulkijniwat, A. (2010), "Analysis of strength development in cement-stabilised silty clay based on microstructural considerations", *Constr. Build. Mater.*, **24**(10), 2011-2021. https://doi.org/10.1016/j.conbuildmat.2010.03.011.
Horpibulsuk, S., Rachan, R. and Suddeepong, A. (2011), "Assessment of strength development in blended cement admixed Bangkok clay", *Constr. Build. Mater.*, **25**(4), 1521-1531. https://doi.org/10.1016/j.conbuildmat.2010.08.006.
Horpibulsuk, S., Phojan, W., Suddeepong, A., Chinkulkijniwat, A. and Liu, M.D. (2012), "Strength development in blended cement admixed saline clay", *Appl. Clay Sci.*, **55**, 44-52. https://doi.org/10.1016/j.clay.2011.10.003.
Jamsawang, P., Nuansrithongb, N., Voottipruexc, P., Songpiriyakijd, S. and Jongpradiste, P. (2017), "Laboratory investigations on the swelling behavior of composite expansive clays stabilised with shallow and deep clay-cement mixing methods", *Appl. Clay Sci.*, **148**, 83-94. https://doi.org/10.1016/j.clay.2017.08.013.
Jiang, H., Wang, B., Inyang, H.I., Liu, J., Gu, K. and Shi, B. (2013), "Role of expansive soil and topography on slope failure and its countermeasures, Yun county, China", *Eng. Geol.*, **152**, 155-161. https://doi.org/10.1016/j.enggeo.2012.10.020.
Jiang, M., Li, T., Cui, Y. and Zhu, H. (2017), "Mechanical behavior of artificially cemented clay with open structure: Cell and physical model analyses", *Eng. Geol.*, **221**, 133-142. https://doi.org/10.1016/j.enggeo.2017.03.002.
Julphunthong, P., Thongdetsri, T. and Chompoorat, T. (2018), "Stabilisation of soft Bangkok clay using Portland cement and calcium sulfoaluminate-belite cement", *Key Eng. Mater.*, **775**, 582-588. https://doi.org/10.4028/www.scientific.net/KEM.775.582.
Khan, M.S., Hossain, S., Ahmed, A. and Faysal, M. (2017), "Investigation of a shallow slope failure on expansive clay in Texas", *Eng. Geol.*, **219**, 118-129. https://doi.org/10.1016/j.enggeo.2016.10.004.
Khattab, S.A., Al-Mukhtar, M. and Fleureau, J.M. (2007), "Long-term stability characteristics of a lime-treated plastic soil", *J. Mater. Civ. Eng.*, **19**(4), 358-366. https://doi.org/10.1061/(ASCE)0899-1561(2007)19:4(358).
Komin, H. and Ogata, N. (1996), "Prediction for swelling characteristics of compacted bentonite", *Can. Geotech. J.*, **33**(1), 11-22. https://doi.org/10.1139/t96-021.
Locat, J., Berube, M.A. and Choquett, M. (1990), "Laboratory investigations on the lime stabilization of sensitive clays: Shear strength development", *Can. Geotech. J.*, **27**(3), 294-304. https://doi.org/10.1139/t90-040.
Mase, L.Z., Likitlersuang, S. and Tobita, T. (2019), "Cyclic behavior and liquefaction resistance of Izumio sands in Osaka, Japan", *Mar. Georesour. Geotec.*, **37**(7), 765-774. https://doi.org/10.1080/1064119X.2018.1485793.
Mutaz, E. and Dafalla, M. (2014), "Utilizing chemical treatment in improving bearing capacity of highly expansive clays", *Proceedings of the Geo-Hubei 2014 International Conference on Sustainable Civil Infrastructure*, Hubei, China, July. https://doi.org/10.1061/9780784478486.010.
Nelson, J.D. and Miller, J.D. (1997), *Expansive Soils: Problems and Practice in Foundation and Pavement Engineering*, John Wiley and Sons, New York, U.S.A.
Nicholson, P.G. (2015), *Soil Improvement and Ground Modification Methods*, Butterworth-Heinemann, Waltham, U.S.A.
Osinubi, K.J. (2000), "Stabilization of tropical black clay with cement and pulverized coal bottom ash admixture", *Adv. Unsatur. Geotech.*, **2000**, 289-302. https://doi.org/10.1061/40510(287)20.
Phanikumar, B.R. (2009), "Effect of lime and fly ash on swell, consolidation and shear strength characteristics of expansive clays: A comparative study", *Geomech. Geoeng.*, **4**(2), 175-181. https://doi.org/10.1080/17486020902856983.
Por, S., Likitlersuang, S. and Nishimura, S. (2015), "Investigation of shrinkage and swelling behavior of expansive/non-expansive clay mixtures", *Geotech. Eng.*, **46**(1), 117-127.
Por, S., Nishimura S. and Likitlersuang, S. (2017), "Deformation characteristics and stress responses of cement-treated expansive clay under confined one-dimensional swelling", *Appl. Clay Sci.*, **146**, 316-324. https://doi.org/10.1016/j.clay.2017.06.022.
Puppala, A.J., Balakrishna, K. and Hoyos, L.R. (2004), "Volumetric shrinkage strain measurements in expansive soils using digital imaging technology", *Geotech. Test. J.*, **27**(6), 547-556. https://doi.org/10.1520/GTJ12069.
Rao, S.M. and Shivananda, P. (2005), "Compressibility behavior of lime-stabilised clay", *Geotech. Geol. Eng.*, **23**, 309-319. https://doi.org/10.1007/s10706-004-1608-2.
Seed, H.B., Woodward, R.J. and Lundgren, R. (1962), "Prediction of swelling potential for compacted clays", *J. Soil Mech. Found. Div.*, **88**(3), 53-87. https://doi.org/10.1061/TACEAT.0008724.
Sharma, N.K., Swain, S.K. and Sahoo, U.C. (2012), "Stabilization of a clayey soil with fly ash and lime: A micro level investigation", *Geotech. Geol. Eng.*, **30**(5), 1197-1205. https://doi.org/10.1007/s10706-012-9532-3.
Sivapullaiah, P.V., Sridharan, A. and Ramesh, H.N. (2000), "Strength behavior of lime treated soils in the presence of sulphate", *Can. Geotech. J.*, **37**(6), 1358-1367. https://doi.org/10.1139/t00-052.
Souza, R.F.C. and Pejon, O.J. (2020), "Pore size distribution and swelling behavior of compacted bentonite/claystone and bentonite/sand mixtures", *Eng. Geol.*, **275**, 20. https://doi.org/10.1016/j.enggeo.2020.105738.
Sun, H., Weng, Z., Liu, S., Geng, X., Pan, X., Cai, Y. and Shi, L. (2020), "Compression and consolidation behaviors of lime-treated dredging slurry under vacuum pressure", *Eng. Geol.*, **270**, 5. https://doi.org/10.1016/j.enggeo.2020.105573.
Tastan, E.O., Edil, T.B., Benson, C.H. and Aydilek, A.H. (2011), "Stabilization of organic soils with fly ash", *J. Geotech. Geoenviron. Eng.*, **137**(9), 819-833. https://doi.org/10.1061/(ASCE)GT.1943-5606.0000502.
Thay, S., Likitlersuang, S. and Pipatpongsa, T. (2013), "Monotonic and cyclic behavior of Chiang Mai sand under simple shear mode", *Geotech. Geol. Eng.*, **31**(1), 67-82. https://doi.org/10.1007/s10706-012-9563-9.
Thomas, G. and Rangaswamy, K. (2020), "Strengthening of cement blended soft clay with nano-silica particles", *Geomech.*

Eng., **20**(6), 505-516.
http://doi.org/10.12989/gae.2020.20.6.505.

Türköz, M. (2019), "Delayed compaction effect on the strength and dynamic properties of clay treated with lime", *Geomech. Eng*., **18**(5), 471-480.
http://doi.org/10.12989/gae.2019.18.5.471.

Verástegui-Flores, R.D., Di Emidio, G. and Van Impe, W.F. (2010), "Small-strain shear modulus and strength increase of cement-treated clay", *Geotech. Test. J*., **33**(1), 62-71.
https://doi.org/10.1520/GTJ102354.

Wayne, A.C., Osman, M.A. and Ali, E.M. (1984), "Construction on expansive soil in Sudan", *J. Constr. Eng. Manag*., **110**(3), 359-374.
https://doi.org/10.1061/(ASCE)0733-364(1984)110:3(359).

Wei, L., Xu, Q., Wang, S., Wang, C. and Chen, J. (2019), "Development of transparent cemented soil for geotechnical laboratory modelling", *Eng. Geol*., **262**, 28.
https://doi.org/10.1016/j.enggeo.2019.105354.

Yoobanpot, N., Jamsawang, P. and Horpibulsuk, S. (2017), "Strength behavior and micro- structural characteristics of soft clay stabilised with cement kiln dust and fly ash residue", *Appl. Clay Sci*., **141**, 146-156.
https://doi.org/10.1016/j.clay.2017.02.028.

Yoobanpot, N., Jamsawang, P., Poorahong, H., Jongpradist, P. and Likitlersuang, S. (2020), "Multiscale laboratory investigation of the mechanical and microstructural properties of dredged sediments stabilized with cement and fly ash", *Eng. Geol*., **267**, 20. https://doi.org/10.1016/j.enggeo.2020.105491.

Zaimoglu, A.S., Tan, O. and Akbulut, R.K. (2015), "Optimization of consistency limits and plasticity index of fine-grained soils modified with polypropylene fibers and additive materials", *KSCE J. Civ. Eng*., **20**(2), 662-669.
https://doi.org/10.1007/s12205-015-0540-8.

CC